

Demonstration of a multiwave coherent holographic beam combiner in a polymeric substrate

H. N. Yum and P. R. Hemmer

Department of Electrical Engineering, Texas A&M University, College Station, Texas 77843

A. Heifetz, J. T. Shen, J.-K. Lee, R. Tripathi, and M. S. Shahriar

Department of Electrical and Computer Engineering, Northwestern University, Evanston, Illinois 60208

Received April 22, 2005; revised manuscript received July 6, 2005; accepted July 9, 2005

We demonstrate an efficient coherent holographic beam combiner (CHBC) that uses angle multiplexing of gratings in a thick polymeric substrate. Our experimental results compare well with the theoretical model based on the coupled-wave theory of multiwave mixing in a passive medium. A CHBC of this type may prove useful in producing a high-power laser by combining amplified beams produced by splitting a master oscillator. Furthermore, the ability to angle multiplex a large number of beams enables a CHBC to be used in multiple-beam interferometry applications as a high-precision surface sensor. © 2005 Optical Society of America

OCIS codes: 050.7330, 090.7330.

In recent years there has been a keen interest in producing high-power lasers by using the method of beam combination. For some applications, such as a Doppler laser radar, it is necessary to ensure that the combined output is spectrally narrow. This requirement can be met by use of a coherent beam combiner (CBC).¹⁻⁶ For example, to circumvent the damage threshold as well as the saturation constraints of optical amplifiers, one can first split a master oscillator into N copies, each of which is then amplified without affecting their mutual coherences. The amplified beams are then combined by the CBC. In principle, an $N \times 1$ CBC system with amplification can be implemented with a tree of conventional beam splitters, as shown in Fig. 1A.⁴ At every node of the tree there is a 50/50 beam splitter. The same tree of beam splitters operating in reverse combines the beams. Maximum output is ensured by phase locking, which can be implemented with electro-optic modulators with feedback, for example. However, a much more robust system that requires fewer optical components can be constructed with coherent holographic beam combiners (CHBCs), as shown in Fig. 1B. In addition, a CHBC can be used as a high-precision surface sensor, as discussed below. A CHBC is a holographic structure with N superimposed common-Bragg-angle gratings that one can prepare by recording the holograms sequentially, with the reference wave incident at a fixed angle and the object wave incident at a different angle for each of the N exposures.^{1,7}

In this Letter we demonstrate a CHBC that uses volumetric multiplexing of gratings in a thick polymeric substrate. Our experimental results compare well with the theoretical model based on the coupled-wave theory of multiwave mixing in phase gratings.⁸⁻¹² We assume that the gratings are recorded in a lossless dielectric material by plane

waves propagating in the $x-z$ plane and polarized in the y direction. We restrict our analysis to the Bragg-matching condition; the coupled-wave equations are $C_R \partial R / \partial z = -j \sum \kappa_m S_m$ and $C_{S_m} \partial S_m / \partial z = -j \kappa_m R$. Here R and S_m are the amplitudes of the reference and the m th diffracted waves, respectively. We define the obliquity factors C_R for the reference and C_{S_m} for the m th diffracted waves as $C_R = \rho_z / \beta$ and $C_{S_m} = \sigma_{mz} / \beta$, where ρ and σ_m are the corresponding wave vectors and β is the propagation constant. The coupling constant is $\kappa_m = \pi n_m / \lambda$, where n_m is the amplitude of spatial modulation of the refractive index. The m th grating is characterized by grating strength $\nu_m = \pi n_m d / [\lambda (C_R C_{S_m})^{1/2}]$, where d is the thickness of the material. We define the diffraction efficiency of the m th grating by $\eta_m = (|C_{S_m} / C_R| S_m(d) S_m^*(d))$.

In the beam-splitter mode, input wave R illuminates N superimposed gratings at the common Bragg angle and couples into diffracted waves $S_1 \dots S_N$. The waves produced by the CHBC have equal and maximum diffraction efficiencies when the N grating

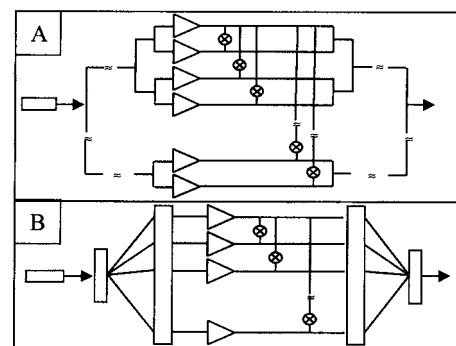


Fig. 1. A, $N \times 1$ CBC implemented with a tree of conventional 50/50 beam splitters. B, $N \times 1$ CHBC (\triangleright , amplifier; \otimes , phase lock).

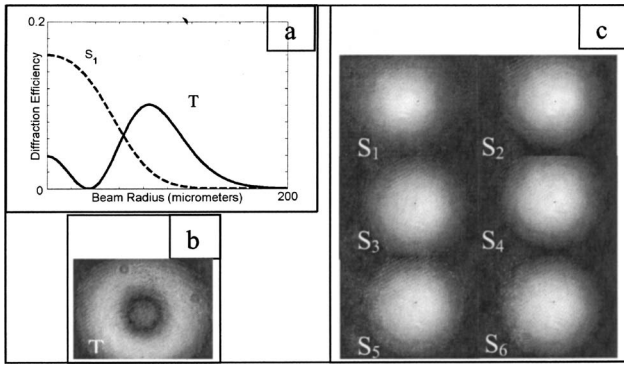


Fig. 2. a, Numerical simulations of beam profiles' relative diffraction efficiency η/η_0 as a function of beam radius [μm]. $\nu=0.23\pi$ for T and S_1 . Beam profiles of $S_2\dots S_6$ are similar to that of S_1 . b, c, Experimentally observed beam profiles for the transmitted T and diffracted beams $S_1\dots S_6$ for the six-beam splitter.

strengths satisfy the condition $(\sum \nu_m^2)^{1/2} = \pi/2$. Therefore the optimal grating strengths are $\nu_1 = \nu_2 = \dots = \nu_N = \nu = \pi/2\sqrt{N}$. From time-reversal symmetry of Maxwell's equations, it follows that a beam combiner must show maximum diffraction efficiency for the same grating strengths that would yield maximum diffraction efficiencies for the beam-splitter mode. The boundary conditions for the gratings in a beam-splitter mode at $z=0$ can be written as $R(0)=1$ and $S_1(0)=S_2(0)=\dots=S_N(0)=0$. The solutions of the differential equations at $z=d$ are $R(d)=\cos(\sqrt{N}\nu)$ and $S_m(d)=-j(1/\sqrt{N})\sin(\sqrt{N}\nu)$.

In the beam-combiner mode the waves $S_1\dots S_N$ illuminate the superimposed gratings, each at the corresponding Bragg angle, thus producing a combined diffracted wave R . In the presence of a linear phase delay between the N input waves, the boundary conditions at $z=0$ are $R(0)=0$, $S_1(0)=1$, $S_2(0)=\exp(j\phi)$, $S_3(0)=\exp(j2\phi)$, and $S_4(0)=\exp(j3\phi)\dots S_N(0)=\exp[j(N-1)\phi]$, where ϕ is the phase delay. Defining $\gamma = \sum (\Pi C_{S_m}) \kappa_m^2 / C_{S_m}$, we obtain the solution at $z=d$ to be given by $R(d) = -j[\Pi C_{S_m} / (C_R \gamma)]^{1/2} \{\sum \kappa_m \exp[j(m-1)\phi]\} \sin[(\gamma/\Pi C_{S_m})^{1/2} d]$. The intensity of the output wave of a beam combiner is $I=R(d)R^*(d)$.

Our holograms were written and read with a frequency-doubled cw Nd:YAG laser operating at 532 nm. We recorded six angle-multiplexed holograms in the photopolymer-based Memplex thick holographic material developed by Laser Photonics Technology, Inc.¹³ The incident angle of reference wave R was held constant during every exposure. Beams $S_1\dots S_6$ were recorded at fixed angular intervals. During the readout, reference beam R illuminated the holograms at the common Bragg angle, and beams $S_1\dots S_6$ were reconstructed simultaneously. The numerical simulation results for beam profiles are presented in Fig. 2a. Figures 2b and 2c show the experimental transmitted (T) and diffracted beam profiles. We estimated the value of $\nu=0.23\pi$ by fitting the numerical simulation curves to the experimentally observed beam profiles. This value is only

slightly larger than $\nu=\pi/2\sqrt{6}\approx 0.204\pi$, at which the maximum diffraction efficiency is achieved.

The optical setup for demonstrating a six-beam combiner is presented in Fig. 3. The input beam from the laser illuminates the hologram in the direction of reference R . The gratings act as a beam splitter, producing six diffracted waves (indicated by solid lines in the figure). The six waves are collimated by a lens and reflected by a tilted mirror. The lens is placed a focal length away from both the CHBC and the mirror to create a $4f$ imaging system. The mirror is rotated with a piezoelectric element by a small angle to vary the phase delay. The angle is small enough that the reflected beams remain Bragg matched. Phase delay ϕ between the adjacent waves is a constant for a given angle of the mirror. The six reflected waves illuminate the hologram in the beam-combiner mode. The combined beam is partially reflected by a 60% reflecting beam splitter and monitored by a photodetector.

Figure 4 (top) shows the numerical simulations of the equations above for the output intensity of a six-beam combiner with unit intensity input beams as a function of phase delay ϕ for three values of ν , 0.204π , 0.123π , and 0.08π . The intensity profile obtained by solution of the coupled-wave equations resembles the familiar multiple-beam interference pattern. We estimate the finesse (F) of the CHBCs by dividing the peak-to-peak angular bandwidth [called the free angular range (FAR)] by the half-peak intensity angular bandwidth ($\Delta\phi_{1/2}$). Whereas the maximum intensity varies as a function of ν , all three cases have the same finesse value, $F=6$. Note that this value is the same as that of N , the number of beams combined, as is to be expected because the finesse of any resonator is directly related to the number of beams that contribute to the peak of the interference curve. Figure 4 (bottom) shows the intensity of the partially reflected combined beam measured by the photodetector. We estimate the finesse of this six-beam combiner to be 5.7, which is very close to the theoretical value of 6.

We denote by I_0 the sum of the intensities of diffracted beams $S_1\dots S_6$ measured just after the CHBC when it is operating as a beam splitter. As $\nu=0.23\pi$ for our CHBC, the peak of the output intensity of the

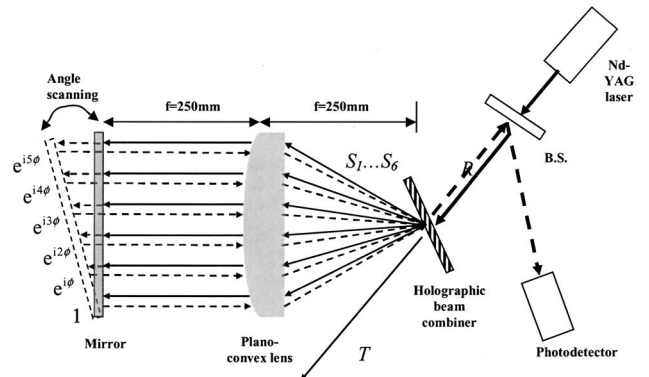


Fig. 3. Six-beam splitter-combiner experiment. The scanning angle is very small, so the reflected beams are Bragg matched.

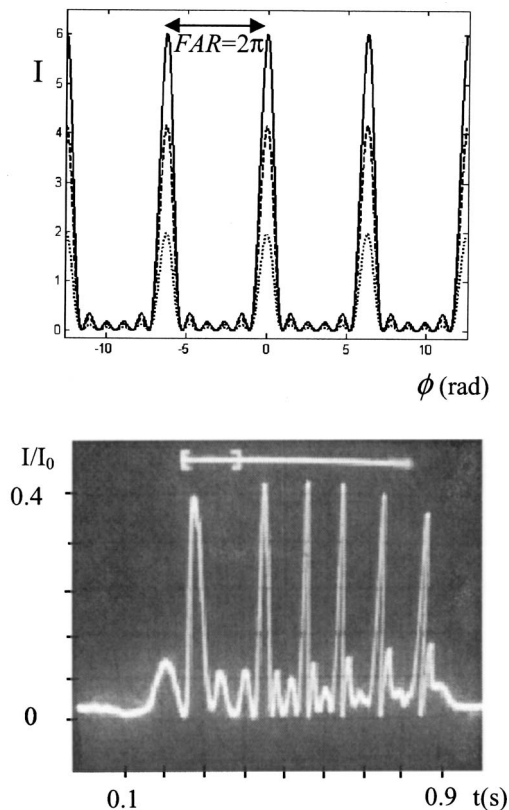


Fig. 4. Top, simulation results for the intensity of the output wave of a six-beam combiner with unit intensity input beams as a function of phase delay ϕ for three values of ν . Solid curve, $\nu=0.204\pi$; dashed curve, $\nu=0.123\pi$; dotted curve, $\nu=0.08\pi$. Bottom, intensity measured by a photodetector in the experimental setup shown in Fig. 3. The difference in spacing between the peaks is due to a slight nonlinearity in the angle scan.

six-beam combiner was calculated to be $0.97I_0$. Because we used a 60% reflection beam splitter, the detected intensity of the output beam from the six-beam combiner, corrected for the Fresnel reflection from the hologram's surface, was expected to be $\sim 0.5I_0$. However, the height of the largest peak in Fig. 4 (bottom) was measured to be $\sim 0.4I_0$. The discrepancy from the theoretically expected value is perhaps attributable to the residual imperfections in the experimental process as well as to the inherent assumptions in the coupled-wave theory analysis. For example, whereas the theoretical model assumes the use of plane waves, the actual beams employed had transverse intensity distributions that are Gaussian in nature. In addition, the analysis assumes perfect Bragg matching, which is difficult to achieve experimentally.

As we described above, a CHBC may be useful in producing high-power laser beams. In addition, a CHBC may find applications as a high-precision surface sensor. For instance, if we replace the rotating mirror with some unknown specularly reflecting surface in the experimental setup in Fig. 3, we can use the CHBC to perform a multiple-beam interferomet-

ric study of the unknown surface. Sharp fringes can be obtained with multiple-beam interferometry, thus providing a much higher resolution than that achievable with simple two-beam interferometry. For example, one can detect unknown surface displacement D by observing a shift of the fringes with an accuracy limited by $(\text{SNR})\Delta D = (\lambda F)/\sigma$, where σ is the signal-to-noise ratio. Previously reported holographic multiple-beam interferometry techniques relied on the nonlinear properties of the holographic material, thus generating the beams as multiple diffraction orders.^{14–17} Using a CHBC made with volume gratings allows for interferometry with a much higher number of beams (~ 1000) and, therefore, higher precision in measurements.¹⁸ In addition, it is possible to make a CHBC by angle multiplexing beams in horizontal and vertical directions and thus to obtain two-dimensional information about the vibrating surface.

To summarize, we have demonstrated a CHBC for six beams at 532 nm that uses volumetric multiplexing of gratings in a thick polymeric substrate. Our experimental results compare well with the theoretical model based on the coupled-wave theory of multi-wave mixing in a passive medium.

This study was supported in part by U.S. Air Force Office of Scientific Research grant FA49620-03-1-0408. A. Heifetz's e-mail address is heifetz@ece.northwestern.edu.

References

1. M. S. Shahriar, J. Riccobono, M. Kleinschmit, and J. T. Shen, *Opt. Commun.* **220**, 75 (2003).
2. J. Zhao, X. Shen, and Y. Xia, *Opt. Laser Technol.* **33**, 23 (2001).
3. J. Harrison, G. A. Rines, and P. F. Moulton, *Opt. Lett.* **13**, 111 (1988).
4. G. L. Schuster and J. R. Andrews, *Opt. Lett.* **18**, 619 (1993).
5. J. Lu, Z. Shen, H. Gao, and Z. Ma, *Opt. Commun.* **244**, 305 (2005).
6. M. Sprenger, Y. Ding, P. Pogany, P. Roentgen, and H.-J. Eichler, *Opt. Lett.* **22**, 1147 (1997).
7. L. Solymar and D. J. Cooke, *Volume Holography and Volume Gratings* (Academic, 1981).
8. H. Kogelnik, *Bell Syst. Tech. J.* **48**, 2909 (1969).
9. S. K. Case, *J. Opt. Soc. Am.* **65**, 724 (1975).
10. R. Magnusson and T. K. Gaylord, *J. Opt. Soc. Am.* **67**, 1165 (1977).
11. J. Zhao, P. Yeh, M. Khoshnevisan, and I. McMichael, *J. Opt. Soc. Am. B* **17**, 898 (2000).
12. H. Kobolla, J. Schmidt, J. T. Sheridan, N. Streibl, and R. Völkel, *J. Mod. Opt.* **39**, 881 (1992).
13. R. Burzynski, D. N. Kumar, M. K. Casstevens, D. Tyczka, S. Ghosal, P. M. Kurtz, and J. F. Weibel, in *Proc. SPIE* **4087**, 741 (2000).
14. K. Matsumoto, *J. Opt. Soc. Am.* **59**, 777 (1969).
15. O. Bryngdahl, *J. Opt. Soc. Am.* **59**, 1171 (1969).
16. W. Schumann, *Holographic and Deformation Analysis* (Springer-Verlag, 1985).
17. K. Matsuda, Y. Minami, and T. Eiju, *Appl. Opt.* **31**, 6603 (1992).
18. F. H. Mok, *Opt. Lett.* **18**, 915 (1993).